

RSC Advances



This is an *Accepted Manuscript*, which has been through the Royal Society of Chemistry peer review process and has been accepted for publication.

Accepted Manuscripts are published online shortly after acceptance, before technical editing, formatting and proof reading. Using this free service, authors can make their results available to the community, in citable form, before we publish the edited article. This *Accepted Manuscript* will be replaced by the edited, formatted and paginated article as soon as this is available.

You can find more information about *Accepted Manuscripts* in the [Information for Authors](#).

Please note that technical editing may introduce minor changes to the text and/or graphics, which may alter content. The journal's standard [Terms & Conditions](#) and the [Ethical guidelines](#) still apply. In no event shall the Royal Society of Chemistry be held responsible for any errors or omissions in this *Accepted Manuscript* or any consequences arising from the use of any information it contains.

Table of Contents

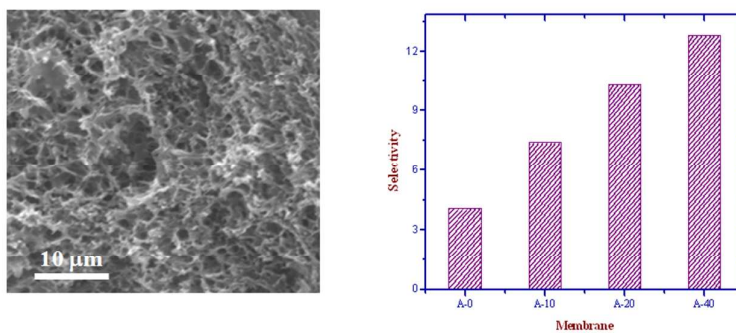


Figure 1: Cross-section SEM image and selectivity for novel positively charged organic-inorganic hybrid ultrafiltration membranes

Positively charged organic-inorganic hybrid ultrafiltration membranes for selective protein separation were fabricated from blends of PVA, functionalized chitosan and tetraethylorthosilicate.

Functionalized chitosan derived novel positively charged organic-inorganic hybrid ultrafiltration membranes for protein separation

Mahendra Kumar, Declan McGlade and Jenny Lawler*

Membrane Technology Laboratory, School of Biotechnology, Dublin City University, Dublin 9, Ireland.

* *E-mail:* jenny.lawler@dcu.ie, **Tel:** +353 1 700 5394; **Fax:** +353 1 700 5412.

Abstract

Novel positively charged organic-inorganic hybrid ultrafiltration membranes with adjustable charge density were fabricated from blends of water soluble poly vinyl alcohol (PVA) and methylated N-(4-N,N-dimethylaminobenzyl) chitosan (TMBC) in combination with tetraethyl orthosilicate (TEOS) silica precursor by the sol-gel method and precipitation in a mixture of methanol and water (80 wt%: 20 wt%). The porous hybrid membrane morphologies, structures, charge and surface properties were characterized comprehensively using scanning electron microscopy, Fourier transform infrared spectroscopy in the attenuated total reflection mode, outer surface zeta potential and contact angle measurements. The results confirmed that the fabricated membranes were porous, hydrophilic and mildly charged in nature. The water flux and flux recovery ratio (i.e. protein fouling resistance) of the membranes were highly dependent on the fraction of TMBC. The protein transmission as a function of *pH* and the fraction of TMBC was studied for two model proteins (ovalbumin; OVA and lysozyme; LYZ) and found to be controlled by size exclusion and the membrane charge density (controlled by the fraction of TMBC). The highest transmission of proteins at their isoelectric points was obtained for the membrane with 40 wt% of TMBC. The best separation of LYZ from OVA in the model mixture solution was obtained at *pH* = 11 when membrane A-40 was used in ultrafiltration of protein solution at 2 bar applied transmembrane pressure.

Introduction

Separation and recovery of proteins are important processes in food, pharmaceutical and biotechnological industries. Research on protein separation and recovery is driven by the increasing demand for high-purity therapeutic proteins in the biopharmaceutical industry.¹⁻² However, protein separation can be a difficult process due to the complexity of the proteins themselves and their biological environments; therefore, the separation and purification often accounts for a major proportion of the production cost. Conventional separation techniques such as affinity separation, chromatography and electrophoresis have been successfully used in pharmaceutical and biotechnological industries.²⁻⁴ These processes are not inherently suitable for large-scale exploitation because of their low throughput, high cost and difficulties in scaling up.

Several researchers have explored adsorption⁵, ultrafiltration⁶, membrane adsorber⁷, microfluidic⁸ and electrophoretic membrane contactor⁹ technologies to separate and recover proteins from their mixture model solutions and biological samples. Among the aforementioned separation processes, ultrafiltration (UF) has been demonstrated in concentration and purification as well as separation of protein mixtures in model solutions and fermentation broths because this process does not require large quantities of salts and buffers, and offers continuous operation, eliminating some of the troublesome aspects of chromatography.¹⁰⁻¹² The major obstacle in UF of protein solutions is membrane fouling which occurs due to nonspecific adsorption and deposition of proteins on the membrane surface or in pores.^{10,12,13} Thus, there is an urgent need to reduce membrane fouling for their practical applications in UF of protein solutions at a specific *pH*. A variety of technologies have been explored for reduction of membrane fouling, including the coating of block copolymers on the membrane surface¹⁴, blending of hydrophobic polymers with hydrophilic copolymers¹⁵ and the covalent grafting of functional hydrophilic polymers onto the

hydrophobic membrane surface by polymerization using ultra-violet light⁷, click chemistry approach¹⁶, electron-beam-induced grafting method¹⁷, and atom transfer radical polymerization⁷. However, the surface-coated layer of block copolymers is physically bound on the membrane surface and therefore it is relatively easily washed off. Grafting of polymers on the membrane surface is responsible for variations in barrier pore size and distribution, leading to a decline in the permeability of the modified membranes.^{7,17} Due to these reasons, blending of hydrophilic polymer/block copolymer with hydrophobic membrane forming polymers seems to be a more promising and efficient approach for preparation of low fouling UF membranes for protein solution ultrafiltration by non-solvent induced separation methods. Previously prepared membranes have shown that the hydrophilicity of the fabricated membranes was improved and their selectivity was low with proteins.^{15,18}

The hydrophilicity and selectivity of the membranes toward proteins have been improved when charged (anionic or cationic) groups have been anchored in the barrier layer of the membranes. The charged groups in the barrier layer of the membranes have been anchored by blending of hydrophobic polymers with functionalized hydrophilic polymers, chemical modification of membranes using the functionalized ligands or by conducting the sol-gel reaction in acidic conditions using water soluble unfunctionalized polymer (i.e. PVA) and functionalized polymers (phosphonated and quaternized chitosan) to fabricate organic-inorganic hybrid materials.^{6,11,12,19-21} PVA has been studied extensively as a membrane material due to its high hydrophilicity, excellent film forming properties, low cost, commercial availability and chemical resistance as well as reactive functional groups for further cross-linking by irradiation, chemical, or thermal treatments.²²

Hybrid organic-inorganic membrane materials have been developed as a promising alternative to conventional organic or inorganic membrane materials. More specifically, organic-inorganic hybrid membranes, in which the organic and inorganic components are

linked together through strong ionic/covalent bonding have gained significant research interest because of better dispersion and stronger bonding between organic and inorganic moieties.^{21,23,24} In particular, much interest has been recently dedicated to design charged organic-inorganic hybrid membranes for ultrafiltration²¹ pervaporation²³ and electro-membrane separation process.²⁴ Water soluble derivatives of chitosan have also been used in the fabrication of low fouling charged UF membranes by non-solvent phase inversion method. The membranes showed low protein fouling and improved selectivity towards proteins.^{19,25} Saxena et al. have reported negatively and positively charged organic-inorganic hybrid UF membranes for the separation of binary mixtures of proteins (bovine serum albumin and LYZ) solution. The separation of bovine serum albumin or LYZ from their binary mixture model solutions was achieved at their isoelectric point when charged membranes were used in UF of mixed proteins solution.²¹ Recently, Qiu et al. have fabricated positively charged UF membranes from the self-assembly of amphiphilic polystyrene-*b*-poly-4-vinylpyridine block copolymer. Subsequently, the quaternary ammonium groups in the barrier layers of the membranes were anchored by conducting the heterogeneous quaternization reaction using 2-chloroacetamide. The selectivity of the membranes in separation of bovine serum albumin from haemoglobin in a mixture model solution was enhanced 10 times compared to conventional UF membranes.²⁶ The combination of size- and charge-based selectivity enhances the separation performance of UF membranes. The transport of proteins across the charged UF membranes is also dependent on the type and strength of electrostatic interactions between the membrane and the protein at a specific solution *pH*.^{6,11,12,27}

Thus, selective separation and purification of protein mixtures solution using charged UF membranes is, in principle, possible at a controlled *pH* and applied transmembrane pressure. By considering the above facts, in this study, positively charged organic-inorganic hybrid UF

membranes have been fabricated by the sol-gel and precipitation method followed by chemical cross-linking using formaldehyde in acidic solution from a water soluble derivative of chitosan; methylated N-(4-N,N-dimethylaminobenzyl) chitosan, tetraethyl orthosilane and PVA. A water soluble derivative of chitosan was used to anchor the quaternary ammonium groups in the barrier layer of the membranes, while PVA was used to improve the mechanical strength. To the best of our knowledge, TMBC derived positively charged organic-inorganic hybrid UF membranes for protein separation applications have not been reported previously. The fabricated membranes have been characterized comprehensively and then used in the UF of the model proteins (OVA and LYZ) solution at varied *pH* and constant applied transmembrane pressure.

Experimental Section

Materials

Chitosan ($M_w \sim 200,000$; N-deacetylation degree 75-85%), poly (vinyl alcohol) (PVA; $M_w \sim 61,000$), 4-dimethylaminobenzaldehyde, tetraethyl orthosilicate (TEOS), phenolphthalein, sodium borohydride (NaBH_4) and acetic acid were procured from Sigma-Aldrich Chemicals, Ireland. Ovalbumin (OVA; 45 kg mol^{-1} , isoelectric point; *pI* ~ 4.5) was purchased from Sigma-Aldrich and lysozyme (LYZ; 14 kg mol^{-1} , isoelectric point *pI* ~ 11) was obtained from Fluka Chemicals. Sodium dihydrogen phosphate, disodium hydrogen phosphate, methyl iodide (CH_3I), sodium iodide (NaI), sodium hydroxide and sodium sulfate decahydrate ($\text{Na}_2\text{SO}_4 \cdot 10\text{H}_2\text{O}$) were received from Merck Chemicals. Formaldehyde, acetone and methanol were purchased from VWR Chemicals, Ireland. Other reagents and chemicals were of commercial grade and used as received. Distilled water (DW) and water purified with a Milli-Q system (Millipore) were used in this study.

Synthesis of methylated N-(4-N,N-dimethylaminobenzyl) chitosan

Methylated N-(4-N,N-dimethylaminobenzyl) chitosan (TMBC) was synthesized in two steps according to the reported procedure in literature.²⁸ Initially, N-(4-N,N-dimethylaminobenzyl) chitosan was prepared from chitosan and N,N-dimethylamino benzaldehyde by the Schiff-base formation reaction (**Scheme 1**). In a typical synthetic procedure, 2 g chitosan was dissolved in 1 wt% aqueous acetic acid solution; then 70 ml of absolute ethanol was added into the solution to obtain its dilute solution and the *pH* of the diluted solution was adjusted to 3 using 1 M HCl solution. Thereafter, 3 equivalent of N,N-dimethylamino benzaldehyde to one equivalent of -NH₂ groups of chitosan was added and subsequently, the reaction continued with constant stirring at 30°C for 18 h. The temperature of the reaction mixture was cooled to room temperature (RT) and the *pH* of the mixture solution increased to 5 by adding 1 M NaOH solution. An aqueous solution of NaBH₄ (2.5% w/v) was added drop-wise for the reduction of imine linkage in the modified chitosan (cf. **Scheme 1**). The reduced chitosan derivative was precipitated in acetone; the resulting precipitate was collected by vacuum filtration on filter paper and dried in a vacuum oven at 40°C for 12 h. In the second step of this process, 1 g of N-(4-N,N-dimethylaminobenzyl) chitosan was dispersed into 40 ml N-methyl pyrrolidone at 25°C for 12 h and then 3 g of NaI and 6 ml of 15% NaOH solution added into the suspension. The reaction mixture was stirred at 60°C for 30 min, subsequently, 5 ml of CH₃I in three portions (2:2:1) was added at 3 h intervals. The reaction continued under constant stirring at 60°C for 12 h. The reaction mixture solution turned to transparent and yellow in colour and then 50 ml of 5% w/v NaCl solution was added into the mixture solution. The resulting mixture solution was further stirred at RT for 24 h to convert the quaternized chitosan derivative in iodide form to chloride. The resulting product was precipitated in 300 ml acetone; the precipitate was collected by vacuum filtration on the filter paper and dried in a vacuum oven at 40°C for 12 h. Finally, a light yellow coloured powder

obtained which was highly water soluble in the pH range from 1-12. The FTIR spectrum of TMBC was recorded (Supporting Information, **Fig. S1**). The broad band at 3378 cm^{-1} is attributed to the stretching vibration of O–H groups in TMBC. The absorption bands at 1642 and 1470 cm^{-1} are observed due to the presence of quaternary ammonium; $-\text{N}(\text{CH}_3)_3^+$ groups in modified chitosan derivative and the obtained results confirm the success of TMBC synthesis.²⁸

Membrane preparation

Methylated N-(4-N,N-dimethylaminobenzyl) chitosan, tetraethyl orthosilicate and poly vinyl alcohol derived hybrid membranes were prepared in three steps: (i) sol-gel method, (ii) precipitation and (iii) chemical cross-linking with formaldehyde in acidic condition (**cf. Fig.1**). 10 g of PVA was dissolved in a round bottom flask containing 100 ml of DW with constant stirring at 70°C and 1 g TMBC was dissolved in another round bottom flask containing 50 ml of DW. Thereafter, both polymer solutions were mixed and stirred overnight at RT to obtain a homogeneous polymer blend solution. Then 20 wt% TEOS of the total weight of PVA and TMBC was added into the polymer blend solution and subsequently, the *pH* was adjusted to 2 by adding a few drops of 4 M HCl solution. The resulting mixture solution was further stirred at RT for 12 h to hydrolyze the alkoxy groups in the TEOS and a viscous gel was obtained. The resulting gel was cast onto a clean glass plate using a glass rod with a gap height of $250\ \mu\text{m}$. The transparent light yellow colour membrane with glass plate was left at 30°C for 1 h and then immersed in a coagulation bath containing methanol (80 % w/v) and DW water (20 % w/v) to precipitate the membrane. The temperature of the coagulation bath was kept at 20°C . The resulting membrane was taken out of the coagulation bath after 2 h and kept in a vacuum oven at 25°C for 12 h to evaporate the residual water and solvent. The same procedure was adopted to fabricate the hybrid membranes with a varied fraction of TMBC. The obtained membranes were placed into a solution containing

formaldehyde (54.1 g), sodium sulfate (150 g), sulfuric acid (125 g), and DW (470 g) for effective cross-linking at 60°C for 1 h.^{21,24,29} The prepared membranes were equilibrated in 1 M HCl and NaOH solutions consecutively for 24 h to convert them to OH⁻ form. The acid and base treated membranes were thoroughly washed with DW to remove any traces of acid and base. The clean membranes were stored in DW for further characterization and use. The membranes are designated as membrane A-X (X being the fraction of TMBC (wt%) to the total fraction of PVA (%) i.e. membrane A-0, A-10, A-20 and A-40, respectively).

Characterization

The water uptake (ϕ), porosity (ϵ), ion-exchange capacity (IEC) and fixed ion concentration (A_f) of the membranes were determined according to previously reported methods.^{12,24} The details are given in the supporting information (sections **S1** and **S2**). The attenuated total reflection - Fourier transform infrared (ATR-FTIR) spectrum of the membrane A-40 was recorded on a Perkin Elmer Spectrum 100 spectrometer and the spectrum was recorded over a wide range from 650 to 4000 cm⁻¹ for 32 scans at a resolution of 4 cm⁻¹. The surface and cross-section morphologies of the membranes were studied using a Hitachi S3400N, UK, scanning electron microscope. The dried membrane samples were frozen in liquid nitrogen, fractured and then sputter-coated with gold using a K 550 sputter coater (Emitech, UK) before being observed. The images were recorded using an accelerating voltage of 15 kV with varied magnifications. Differential scanning calorimetry (DSC) studies were conducted to determine the states of water (i.e. total water, free water and bound water) and the thermal stability of the membranes in wet and dry conditions. To determine the states of water, the membrane samples were immersed in DW at RT for 24 h to convert the membranes in a fully swollen state. About 10 mg of wet membrane sample was placed inside the air tight aluminium lid. DSC experiments were then performed using a Q200 series differential scanning calorimeter (TA instrument, USA) in the temperature range from -50 to +50°C

under nitrogen atmosphere with a flow rate of 50 ml/min and a heating rate of 10°C/min. DSC experiments for the dried membranes were performed in the temperature range from 30 to 250°C under similar experimental conditions. A ZetaCAD system (CAD Instruments, France) was used to measure the outer surface zeta potential of the membranes. The details of the experimental conditions are given in a previous paper.³⁰ The streaming potential for each membrane was measured as a function of pressure at varied $pH = 5, 7$ and 10 . The outer surface zeta potential (ζ) of the membranes was calculated using the Helmholtz-Smoluchowsky equation (Eq.(1)):^{10,12}

$$\zeta = \frac{\Delta E_{SP}}{\Delta P} \times \frac{\eta \kappa}{\epsilon_r \epsilon_o} \quad (1)$$

where $\Delta E_{SP}/\Delta P$ is the change in streaming potential with pressure, η is the electrolyte solution viscosity, κ is the conductivity of the electrolyte solution; ϵ_o is the permittivity of free space and ϵ_r is the permittivity of the electrolyte solution. The tensile strength and elongation values at break point were determined using a Zwick Z005 displacement controlled tensile testing machine (Zwick-Roell, Germany) at a crosshead speed of 2 mm/min and the details of the operating conditions are given in the supporting information, **Section S3**. Membrane surface water contact angle measurements were obtained using a sessile drop method on FTÅ 200 contact angle analyzer (First Ten Angstroms, Inc., USA) equipped with video capture. Membrane samples were cut to an appropriate size and carefully mounted on a glass slide using double-sided tape. 2 μ L of deionized water was pumped out from the syringe using the motor-driven micro syringe and dropped onto the membrane sample surface. The direct microscopic measurement for the contact angle between deionized water and membrane surface was determined with the goniometer. For each membrane sample, the contact angle was measured at least five locations on the membrane surface and the reported values are an average of the five measurements. Subsequently, the free energy of interaction at the

interface between the liquid and the membrane surface ($-\Delta G_{SL}$) was calculated using the Young-Dupre equation (Eq. (2)):^{10,12}

$$-\Delta G_{SL} = (1 + \cos \theta) \gamma_L^T \quad (2)$$

where θ is the measured water contact angle and γ_L^T is the total surface tension of water (72.8 mJ m^{-2}).¹⁰

Protein adsorption studies

Static protein adsorption experiments were performed to determine the adsorbed amount of OVA on the membranes at $pH = 3$ and 7 . Circular pieces of membranes (4.9 cm^2 area) were placed into the conical flask together with 25 ml of OVA solution (1 mg ml^{-1}) in 10 mmol phosphate buffer of $pH = 7$. Subsequently, the pH of the solutions was adjusted to 3 and 7 using 1 M HCl/NaOH solutions. The conical flasks were then kept on a shaker at RT for 8 h with a stirring speed of 100 rpm . The membranes were removed from the protein solutions and the concentration of OVA in the supernatant solutions was determined using a Cary 50 Bio UV-Vis spectrophotometer (Varian Inc., USA) at a wavelength of 280 nm . The adsorbed amount of OVA on the membranes was determined from the change in the concentration of OVA before and after adsorption. The reported data are the mean values of triplicate samples for each membrane.

Water flux and ultrafiltration studies

A dead-end stirred ultrafiltration cell (Amicon 8200; Millipore) was used to perform the water and protein solutions ultrafiltration studies at constant applied transmembrane pressure. For the water filtration experiments, each membrane was first compacted by passing DW through the membrane for 30 min at a transmembrane pressure of 3 bar and then the pressure was reduced to 2 bar . Thereafter, DW water was passed through the membranes for 60 min at 2 bar and the mass of the collected permeate (DW) measured on a digital balance (Ohaus

AdventurerTM Pro Balance, UK). The water flux (J_w ; L m⁻² h⁻¹) of the membranes was calculated using Eq. (3):

$$J_w = \frac{m}{A \times \rho \times t} \quad (3)$$

where m is the mass of the collected permeate, ρ is the density of water, A is the membrane area and t is the permeation time. Subsequently, the stirred cell and solution reservoir were emptied and immediately refilled with 500 ml solution of 1 g L⁻¹ OVA. To evaluate the antifouling ability of the membranes, ultrafiltration of OVA solution was performed at $pH = 7$. After ultrafiltration of OVA solution, the membranes were removed from the UF cell and thoroughly washed with DW. The cleaned membranes were again replaced into the cell which was refilled with DW. The water flux of the cleaned membranes was again recorded by passing DW through the membrane for 60 min at 2 bar applied transmembrane pressure. All the ultrafiltration experiments were performed at a stirring speed of 300 rpm. The flux recovery ratio (FRR, in %) of the membranes was determined using Eq. (4):^{12,22}

$$FRR = \frac{J_{wp}}{J_w} \times 100 \quad (4)$$

where J_{wp} is the water flux of the cleaned membrane after UF of OVA solution and J_w is the initial water flux of the membrane.

OVA transmission experiments were performed at $pH = 3, 5$ and 11 and LYZ transmission experiments were performed $pH = 7, 11$ and 12 . 250 ml solution of OVA or LYZ (1 g L⁻¹) of known pH was filled into the stirred cell and UF studies were then performed for 60 min. The concentration of OVA or LYZ in the feed and the permeate samples solutions was determined at a wavelength of 280 nm using a Cary 50 Bio UV-Vis spectrophotometer. The observed transmission of protein (τ_{Obs}) through the membranes was determined using Eq. (5):^{10,31}

$$\tau_{Obs} = \frac{C_p}{C_f} \quad (5)$$

where C_p and C_f are the concentration of protein (OVA or LYZ) in the permeate and feed sample solutions; i.e., no attempts were made to take into account concentration polarization effects that could yield true instead of observed transmission values. The selectivity of the membranes towards LYZ versus OVA was determined by filtering the OVA and LYZ model mixture solutions (1 g L^{-1} each) at $pH = 11$ through the membranes for 60 min. The concentrations of OVA and LYZ in the feed and permeate solutions were determined by sodium dodecyl sulfate polyacrylamide gel electrophoresis (SDS-PAGE) technique.^{11,32} The details of experimental conditions are given in Supporting Information, **Section S4**. The selectivity of membranes towards LYZ versus OVA was calculated using Eq. (6):^{10,31}

$$Selectivity = \frac{(\tau_{Obs})_i}{(\tau_{Obs})_j} \quad (6)$$

where $(\tau_{Obs})_i$ and $(\tau_{Obs})_j$ are the observed transmission values for LYZ and OVA, respectively.

Results and Discussion

The membrane forming material was prepared by the sol-gel method and the condensation polymerization of TEOS in acidic solution containing PVA and TMBC.^{21,29} The pores in the membranes were tailored by precipitation in a binary mixture of non-solvent (DW) and solvent (methanol) for 2 h at 20°C , where DW exchanged with methanol during the precipitation process. The cross-linking of the membranes occurred in two steps: (i) formaldehyde reacted with -OH groups of PVA so that hemiacetal was formed; (ii) hemiacetal reacted with the other -OH group of PVA. Thus acetal was formed in the membrane matrix. The membranes were fabricated at molecular level and PVA, TMBC and TEOS were connected by covalent/hydrogen bonding interaction.^{21,29,33} The schematic structure of the hybrid membranes is shown in **Scheme 2**.

Instrumental and physicochemical characterizations

The ATR-FTIR spectrum for membrane A-40 is presented in **Fig. 2**. The broad absorption band at 3420 cm^{-1} corresponds to the stretching vibration of O-H groups and bound water present in the membrane matrix.^{12,34} The absorption bands at 2918 and 2854 cm^{-1} are observed because of $-\text{CH}_2$ stretching vibrations.³⁴ The absorption band at 1643 cm^{-1} is attributed to the $-\text{N}(\text{CH}_3)_3^+$ groups present in the membranes.^{12,28} The strong absorption band at 1380 cm^{-1} is the characteristic peak for $-\text{C}-\text{O}-\text{C}-$ linkages in the membrane.^{21,33} The absorption band at 1070 cm^{-1} is attributed to the Si-O-Si linkages, while the band at 1012 cm^{-1} is characteristic of Si-O-C linkages in the membranes.^{21,33} The Si-O-Si linkages in the membranes are formed due to the condensation reaction between Si-OH groups from TEOS. The Si-O-C linkages in the membranes due to the condensation reaction between Si-OH groups of TEOS and C-OH groups of PVA.^{21,24,33} The obtained results confirm the successful preparation of positively charged organic-inorganic hybrid UF membranes from PVA, TEOS and TMBC by the sol-gel, precipitation and cross-linking with formaldehyde methods. The DSC thermograms for membranes A-0, A-10, A-20 and A-40 are shown in Supporting Information, **Fig. S2(A)**. Endothermic peaks were obtained for membranes in the temperature range from 140 to 145°C . These peaks are attributed to the evaporation of water from the membranes at elevated temperature. Moreover, the peak area for the membranes was proportionally increased with fraction of TMBC (%). This is ascribed to an increase in water binding capacity of the membranes after the incorporation of TMBC because the fraction of $-\text{N}(\text{CH}_3)_3^+$ groups was proportionally enhanced which have a high capacity to attract water through polar interactions (electrostatic or hydrogen bonding).^{12,35} These results confirm that the prepared membranes are thermally stable. DSC thermograms for the membranes in the water swollen state are depicted in Supporting Information, **Fig. S2(B)**. One melting enthalpy peak for all of the membranes was obtained at $\sim 0^\circ\text{C}$. This could be due to presence of free

water in the membranes. The free water content (ϕ_f ; %) in the membranes was determined using Eq. (7):³⁶

$$\phi_f (\%) = \frac{\Delta H_m}{Q_m} \times 100 \quad (7)$$

where Q_m is the melting enthalpy of water at 0°C (334 Jg⁻¹).³⁶ ΔH_m is the enthalpy of melting for the membrane and its value was obtained from the integration area of melting enthalpy peak for each membrane in the fully swollen state. The bound water content (ϕ_b ; %) was calculated from the difference in total water (ϕ ; %) and free water content (ϕ_f ; %) of the membranes. The obtained values of ϕ_f and ϕ_b for the membranes are tabulated in **Table 1**. The free water content (%) in the membranes decreased, while the bound water content (%) increased with fraction of TMBC (%) because of the proportional increase in the extent of hydrophilic $-\text{N}(\text{CH}_3)_3^+$ groups which are responsible for binding of the water in the channels/pores of the membranes.^{12,35,37} The results demonstrate that the water binding capacity of the membranes was improved after the incorporation of TMBC. The water binding capacity of the membranes could be tuned by varying the fraction of TMBC in the membrane casting solutions. In this study, tensile tests were performed to determine the mechanical strength of the membranes and the measured values of stress (MPa) vs strain (%) are presented in Supporting Information, **Fig. S3**. The value of elongation at break (E_b) for the membranes was obtained from the initial slope of the stress vs strain curves (cf. **Fig. S3**) and these values are presented in **Fig. 3**. E_b values are systematically increased with the fraction of TMBC in the membrane matrix. This could be attributed to: (i) the hydrogen bonding interaction between PVA and TMBC; (ii) the formation of a tight Si-O-Si network in the membrane matrix after the sol-gel reaction under acidic condition and (iii) an increase in the degree of cross-linking of the membranes.^{21,24,38} The E_b value (268 MPa) for membrane A-10 is higher than that of membrane A-0 (202 MPa) because strong hydrogen bonding

occurred between PVA and TMBC and a more effective cross-linking in membrane A-10 due to the availability of more -OH groups on the modified chitosan. The E_b value for membrane A-40 was found to be 425 MPa, which is highest of all the membranes developed (cf. **Fig. 3**). These results show the high tensile and mechanical strengths of the fabricated membranes. The outer surface zeta potential (ζ) values for the membranes at $pH = 5, 7$ and 10 are presented in **Fig. 4**. Membrane A-0 had negative outer surface zeta potentials at the studied pH values. The unfunctionalized membrane A-0 without fixed ionic groups (cf. **Table 1**) became charged due to the adsorption of electrolyte ions; because of the weaker hydration and hence stronger adsorption tendency of anions.^{10,11} However, the outer surface ζ values of the other membranes were positive over the studied pH values. The charge nature of membrane A-10 was tuned because of the surface exposed $-N(CH_3)_3^+$ groups and since the tight hydration layer on the membrane surface, even for lower fraction of TMBC (cf. **Table 1**) did not favour the adsorption of anions at $pH = 5$.^{11,37} The absolute outer surface ζ values for membranes A-10, A-20 and A-40 at $pH = 5$ systematically increased with increasing fraction of TMBC (cf. **Fig. 4**). Moreover, the same trend for the absolute outer surface ζ values of the membrane A-10, A-20 and A-40 were obtained at $pH = 7$ and 10 . On the other hand, these values were lower than that of $pH = 5$ for membranes A-10, A-20 and A-40. Kumar and Ulbricht reported that the outer surface ζ values of the positively charged ultrafiltration membranes depend on the fraction of $-N(CH_3)_3^+$ groups in the membrane matrix.¹¹ Overall, the results confirm positively charged surface and the adjustable charge density on the barrier layer of the fabricated membranes.

The surface and cross-section electron microscopy images of the membranes are presented in **Fig. 5**. The membranes exhibit an asymmetric structure with a dense top (“skin”) layer, and a porous sublayer with fully developed sponge-like structure at the bottom. It can be seen from the cross-sectional SEM images of the membranes (cf. **Fig. 5**) that the porosity of the sub

layer seemed to increase with increasing fraction of TMBC in the casting solutions. This could be correlated to the precipitation rate of membrane forming material in the coagulation bath containing a mixture of methanol and water (80:20 wt%). A lower precipitation rate could provide more time before solidification is reached, enabling nucleation and the growth of the polymer-lean phase to progress further, so that larger pores in spongy like sublayer could be formed during the precipitation process with increasing fraction of hydrophilic TMBC.^{39,40} This phenomenon apparently influenced the formation of the porous membranes with fully developed sponge like structure. The membrane A-40 seemed to have the highest porosity of all of the prepared membranes. The observed water contact angle and the surface free energy values for the membranes are presented in **Fig. 6**. The highest value (75°) of water contact angle and the lowest surface free energy (92 mJ m⁻²) were obtained for membrane A-0, which could be due to the absence of hydrophilic -N(CH₃)₃⁺ groups on the barrier layer of the membrane. Moreover, water contact angle values decreased and the surface free energies increased systematically with increasing fraction of TMBC (%). The hydrophilic -N(CH₃)₃⁺ groups were responsible for the formation of tight hydration layer on the membrane surface through hydrogen bonding between -N(CH₃)₃⁺ groups and water.^{11,37} Hence, the membrane surface became more hydrophilic after the incorporation of TMBC in the membrane matrix. The lowest water contact angle (40°) and the highest surface free energy (128 mJ m⁻²) were obtained for membrane A-40, which correlated with its highest hydrophilicity as deduced from water uptake values and bound water fraction (cf. **Table 1**). The obtained results provide an opportunity for tuning the hydrophilicity of the membranes by varying the fraction of TMBC in the polymer blend casting solutions.

The membranes were characterized physicochemically by determining their water uptake, porosity, ion-exchange capacity and fixed ion concentration (**Table 1**). It was found that the water uptake values increased systematically with increasing fraction of TMBC in the

membranes. This is attributed to the proportional increase in the fraction of $-\text{N}(\text{CH}_3)_3^+$ groups with fraction of TMBC and their strong affinity to attract water through the hydrogen bonding interaction.^{12,37} The porosity values were also increased with fraction of TMBC (cf. **Table 1**) and the highest porosity (66.7%) was obtained for membrane A-40. The *IEC* and *A_f* values were systematically increased with increasing fraction of TMBC because of the proportional increase in the extent of $-\text{N}(\text{CH}_3)_3^+$ groups in the membranes. The *IEC* and *A_f* value for membrane A-40 was found to be 0.70 mequiv. g^{-1} and 1.09 mequiv. g^{-1} H_2O , which are higher than that of other membranes (cf. **Table 1**). However, the *IEC* values of all of the membranes are lower than, for instance, those of other reported positively charged membranes in the literature.^{35,41-43} The relatively low *IEC* and *A_f* values suggest the mildly charged nature of the prepared membranes in this study, which indicates suitability for the selective separation of proteins from binary or ternary protein mixture solutions by ultrafiltration process. Overall, the incorporation of TMBC had an influence on the water binding capacity, the porosity and the charge density (i.e. fixed ion concentration) of the membranes.

Membrane permeability

The water flux (J_w) was measured to evaluate the influence of TMBC fraction on the membrane permeability and the data are presented in **Fig. 7**. The J_w values for membranes gradually increased with fraction of TMBC. This could be attributed to increase in hydrophilicity and porosity of membranes with the same overall morphology and barrier layer thickness. The value of J_w for membrane A-0 was found to be 37.8 $\text{L m}^{-2} \text{h}^{-1}$, which is lower than J_w values for all other membranes. This is due to the lowest water binding capacity and hydrophilicity as well as the porosity of membrane A-0 (cf. **Table 1** and **Fig. 5**). On the other hand, the highest value of J_w (63 $\text{L m}^{-2} \text{h}^{-1}$) was obtained for membrane A-40 because this membrane had highest water binding capacity and hydrophilicity as well as porosity (cf. **Table 1** and **Fig. 5**). It is noted that water flux was highly dependent on the fraction of

TMBC, as a consequence of the bulk and surface charge density contributed by the fraction of TMBC in the membranes (cf. **IEC and A_i; Table 1**). Significant rejection of protein indicated clearly that the prepared membranes were tight UF membranes (e.g., for OVA at $pH = 5$ more than 90% was rejected, corresponding to transmission of less than 0.06; cf. **Fig. 9 (A), below**). The protein solution flux (J_p) values were also dependent on the fraction of TMBC in the membrane (**Fig. 7**); J_p values increased substantially with fraction of TMBC and the highest J_p (OVA; $36 \text{ L m}^{-2} \text{ h}^{-1}$ and LYZ; $48 \text{ L m}^{-2} \text{ h}^{-1}$) values were obtained for membrane A-40. However, J_p values were lower than that of J_w values for all of the membranes, this could be due to concentration polarization and protein fouling which is discussed below in detail. It was further observed that the effective pore size of the barrier layer was almost the same with increasing fraction of TMBC in the membranes because the protein transmission values for some feed conditions even decreased. In addition, the cross-section morphology of the membranes including the “skin” layer thickness is almost similar (cf. **Fig. 5**). Therefore, the observed correlations between membrane structure and performance as a function of increasing fixed ion concentration could mainly be related to the higher porosity and wettability of the barrier layer on the membranes.

Antifouling performance

The antifouling ability of the membranes was evaluated in terms of protein adsorption and flux recovery ratio after ultrafiltration of OVA solution at $pH = 3$ and 7 . In this study, ovalbumin (OVA) was chosen as a model protein. The adsorbed amounts of OVA at $pH = 3$ and 7 are depicted in **Fig. 8(A)**. The adsorbed amounts of OVA at both pH values were reduced for all of the membranes with increasing fraction of TMBC. The obtained trend for adsorption of OVA on the membranes is consistent with the observed water contact angle values (cf. **Fig. 6**). The effective reduction in the adsorbed amount of OVA occurred due to the interaction of OVA with the surface was screened by the tight hydration layer on the

membrane surface due to the polar interactions between $-\text{N}(\text{CH}_3)_3^+$ groups and water.^{12,44} The adsorbed amount of OVA on the membrane A-40 at $pH = 3$ was found to be $15 \mu\text{g cm}^{-2}$, which is ~ 3.5 times lower than that found for the membrane A-0 ($52 \mu\text{g cm}^{-2}$). This could be due to the formation of effective hydration layer on the entire membrane surface by the highest fraction of TMBC and the electrostatic repulsions between positively charged OVA and the positively charged membrane at $pH = 3$. Furthermore, the adsorbed amounts of OVA on the membranes was higher at higher protein solution pH value ($pH = 7$). The effect of solution pH on the adsorption of protein resulted from the change in the electrostatic potential of the protein and the membrane.^{11,45,46} The net charge on OVA changed from positive to negative when the solution pH was tuned from 3 to 7; while the membrane surface remained positively charged. Therefore, the electrostatic attractions between negatively charged OVA (OVA^-) and positively charged membrane surface increased with increasing solution pH above the pI . Thus, the adsorbed amount of OVA on the membranes was higher at $pH = 7$. The adsorbed amount of OVA on the prepared membranes was lower than, for instance, other porous membranes reported in the literature.^{44,47-49} Due to the effective hydration layer on the surface and the electrostatic repulsion between the membranes and protein at $pH < pI$ of OVA, here the reported membranes have a good protein resistance capacity, which is tunable by varying the fraction of TMBC in the casting solutions. The same trend with respect to the adsorbed amount of OVA on the membranes for $pH < pI$ and $pH > pI$ indicated that the repulsion by positively charged groups and the hydration layer was more dominant than that of the electrostatic attraction. Thus, the low fouling positively charged hybrid membranes show the suitability for UF of protein solutions in the studied pH values (cf. **Fig. 9 (A&B)**). The FRR values for membranes after UF of OVA solution at $pH = 3$ are presented in **Fig. 8(B)**. The FRR value for membrane A-0 after UF of OVA solution was found to be 70.6%, which is the lowest value of all of the fabricated membranes. This could be ascribed to

membrane fouling via hydrophobic interaction between OVA and the uncharged membrane surface.^{11,13,48,50} The FRR values for the membranes were further increased with increasing fraction of TMBC and these results can be correlated to the obtained data for the adsorption of OVA on the membranes without UF and the hydrophilicity (cf. **Fig. 6** and **Fig. 8(A)**). In addition, the tight hydration layer on the membrane surface due to the polar interactions between $-N(CH_3)_3^+$ groups and water could substantially suppress the electrostatic interactions between the negatively charged OVA (at $pH = 7$) and the positively charged membrane with fraction of TMBC.^{6,11,13} The FRR value for membrane A-40 was found to be 92 %, which is the highest value of all of the membranes. The obtained high FRR values for positively charged membranes suggest that the adsorbed protein on the membrane surface could be removed easily by physical cleaning i.e. water flushing method.

The transmission of OVA and LYZ

The pH of the protein solution plays an important role in UF separations using charged porous membranes. The electrical charge on the proteins and membranes can be tuned by varying the solution pH due to the presence of acidic or basic groups on the proteins and membranes. The acidic or basic groups ionize as the solution pH is changed and attractive or repulsive interactions are formed between the protein and the membrane surface.^{12,20,27,51} In this study, the change in protein charge was considered to be due to the presence of quaternary ammonium ($-N(CH_3)_3^+$ groups in the barrier layer of the membranes. In addition to OVA, lysozyme (LYZ) was selected as a second model protein because these proteins are major components of chicken egg white.⁵² The transmission of protein (OVA or LYZ) through the membranes in UF at varied pH values was determined and the obtained values are presented in **Fig. 9(A&B)**. The transmission of OVA and LYZ across the membrane A-0 was low because these values were influenced by adsorption and deposition of protein on the unfunctionalized membrane via hydrophobic interactions between them (cf. **Fig. 8(A)** and

Table 1)).^{11,14,50} The transmission of OVA through the membranes was lower in comparison with LYZ under the optimized experimental conditions (cf. **Fig. 9(B)**). This can be well explained on the basis of size difference between OVA and LYZ i.e. OVA is larger than LYZ as indicated by the molecular weights and hydrodynamic radii.^{53,54} The transmission of OVA and LYZ was dependent on the fraction of TMBC and solution *pH* (cf. **Fig. 9(A&B)**). The highest transmission of OVA and LYZ across the membranes was achieved at *pH* = 5 for OVA and *pH* = 11 for LYZ, which corresponds to their *pI* values. The highest absolute transmission values of OVA and LYZ were obtained for membrane A-40 due to its high hydrophilicity and porosity (cf. **Fig. 5 and 6; Table 1**). Furthermore, the charged UF membranes did not create any additional hindrance for the transmission of proteins at their *pI* values and protein fouling was effectively reduced by the tight hydration layer on the membrane surface.^{11,12,20,45} The highest transmission of proteins across the charged UF membranes at their *pI* values had also been reported by other research groups.^{11,20,45} It was found that the transmission of OVA across the membranes was gradually reduced in solution at *pH* = 11 (above *pI* value of OVA) due to the formation of a negatively charged self-rejecting layer of OVA molecules on the membrane surfaces through an electrostatic attraction between the negatively charged OVA and positively charged surface of the membranes.^{11,12,55,56} Thus, the long range electrostatic repulsion between the self-rejecting layer of OVA and OVA molecules in solution was probably responsible for further decline in transmission of OVA at *pH* > *pI* of OVA. Furthermore, the transmission of OVA at *pH* = 3 (below *pI* value of OVA) was lower than the obtained transmission values for all of the membranes at *pH* = 5 and 11, respectively. This can be attributed to the rejection of positively charged OVA by the similar charged membrane surface through an electrostatic repulsion.^{12,13,51,52,56} At *pH* = 3, the transmission of OVA for membrane A-40 found to be lowest (0.015) value because the positively charged OVA excluded in excess during

ultrafiltration by more positively charged barrier layer of the membranes. The transmission of LYZ through the membranes was higher than for OVA at all studied pH values due to its smaller size.⁵⁴ However, the transmission of LYZ across the membranes was very low at $pH = 7$ compared to $pH = 11$ under identical experimental conditions. At $pH = 7$ ($< pI$ of LYZ), LYZ transmission across the membranes was highly hindered due to the strong electrostatic repulsion between the positively charged LYZ^+ and the positively charged membrane surface.^{11,12,20,45} In addition, the transmission of LYZ across the membranes at $pH = 7$ was highly dependent on the fraction of TMBC (cf. **Fig. 9(B)**). The lowest LYZ transmission (0.1) value was achieved for membrane A-40 because of its highest fixed ion concentration in the barrier layer (cf. **Table 1**). On the other hand, the opposite trend was obtained when ultrafiltration of LYZ solution was performed at $pH = 12$. The LYZ transmission values at $pH = 12$ were lower than those at $pH = 11$ (cf. **Fig. 9(B)**). As discussed for OVA previously, the formation of a negatively charged self-rejecting layer of LYZ on the membrane surface seemed to govern the transmission of LYZ at $pH > pI$ of LYZ. Overall, the effect of electrostatic repulsion on the low transmission of proteins (high rejection) was much stronger when the fixed ion concentration in the barrier layer of membrane was dominant (i.e. for LYZ at low pH value). For membrane A-40, the transmission of LYZ was found to be 14 times higher than that of OVA at $pH = 11$. These results suggest the effective possible separation of LYZ from its binary mixture solution with OVA at $pH = 11$ using the positively charged organic-inorganic hybrid ultrafiltration membranes.

Ultrafiltration separation of a binary protein mixture model solution

The UF experiments were performed using a mixed solution of 1 g L^{-1} OVA and LYZ (1:1 ratio) at $pH = 11$ and 2 bar applied transmembrane pressure. SDS-PAGE technique was applied to determine the concentration of OVA and LYZ in the feed and permeate mixture solutions after ultrafiltration (**Fig. 10(A)**). According to the SDS-PAGE marker, the bands at

45 and 14 kDa in the SDS-PAGE patterns represent OVA and LYZ. The thinnest OVA band and the thickest LYZ band were obtained for the permeate protein mixture solution at $pH = 11$. Furthermore, the intensity of the thinnest OVA band and thickest LYZ band varied when ultrafiltration of 1 g L^{-1} OVA and LYZ mixture solution was performed at $pH = 11$ using the membranes with varied fixed ion concentration (cf. **Table 1**). The τ_{Obs} values of OVA and LYZ were directly determined from the SDS-PAGE marker, these values were then used to determine the selectivity of the membranes (cf. **Eq. (6) and Fig. 10 (B)**). It can be seen that the selectivity of the membranes towards LYZ versus OVA was gradually improved with increasing fraction of TMBC because the content of $-\text{N}(\text{CH}_3)_3^+$ groups was proportionally enhanced (cf. **Table 1**). The selectivity of membrane A-10 was found to be 7.5, which is higher than the selectivity of membrane A-0 (4.1). The selectivity of membrane A-10 was high because this membrane did not create any hindrance for passage of neutral LYZ at $pH = 11$ while the transport of OVA at $pH = 11$ could be hindered by the negatively charged self rejecting layer of OVA on the surface of membrane A-10 (cf. above). In addition, there was a chance for the deposition of OVA and LYZ onto the unfunctionalized membrane A-0 during ultrafiltration of protein mixture model solution at $pH = 11$ because of the hydrophobic interaction between the membrane surface and the proteins.^{11-13,48} Therefore, the pore size of the membrane barrier layer could be decreased and thus, the selectivity of membrane A-0 declined. Furthermore, the highest selectivity for LYZ versus OVA was found to be 12.8 for membrane A-40 which is approximately three times higher than that of the unfunctionalized membrane A-0 under the same experimental conditions. The “real” selectivity of membrane A-40 for the protein mixture (12.8) was not much different to the “ideal” selectivity (13.4) determined from the observed transmission for an individual protein (OVA or LYZ) solution. This observation supports strongly the low fouling behaviour and high selectivity of the membranes towards proteins. However, the selectivity of the membranes could be changed if

the concentration gradient between two proteins would be high during ultrafiltration of a protein mixture solution, because a more effective negatively charged self-rejecting layer of OVA ($> pI$ of OVA) could form on the barrier layer of membranes.

Conclusions

Novel positively charged organic-inorganic hybrid ultrafiltration membranes were successfully fabricated from blends of water soluble TMBC, PVA and TEOS by the sol-gel method and precipitation in binary mixture of methanol and distilled water (80 wt% : 20 wt%). The membranes exhibited a relatively dense top (“skin”) layer and a porous sublayer with fully developed sponge-like structure at the bottom of the membranes. The highest membrane porosity, hydrophilicity and fixed ion concentration was obtained for membrane A-40 and these values could be tuned by varying the fraction of TMBC in the membrane casting solutions. The membranes were less prone to protein adsorption and the fouling behaviour was substantially reduced with increasing fraction of TMBC. Thus, protein adsorption and fouling ability of the membranes could be adjusted by varying the fraction of TMBC. Pure water and protein solution fluxes were dependent on the fraction of TMBC in the membranes and the highest values were obtained for membrane A-40. This maximum as a function of TMBC content correlated with those for volume porosity, hydrophilicity and trends in top layer and cross-section morphology observed by electron microscopy. The highest transmissions of OVA and LYZ through the membranes were achieved at $pH = 5$ and 11 , respectively. The best separation of LYZ from OVA in the model protein mixture solution was obtained at $pH = 11$ using the membrane A-40 (i.e. 40% of TMBC to the total weight of PVA), where the high selectivity (12.8) towards LYZ versus OVA was based on the size exclusion and electrostatic repulsion between the negatively charged self rejecting layer of OVA and the negatively charged OVA. The results confirm the suitability of positively charged organic-inorganic hybrid ultrafiltration membranes for the selective

separation of protein from their mixture solution by UF and isoelectric focusing technology. The membranes developed in this study are attractive because of their tunable properties, i.e. relatively low protein fouling and high selectivity towards a specific protein due to the combined size exclusion, effective surface hydration and charge repulsion effects. Also, the trade-off between permeability and selectivity which is commonly observed for conventional UF membranes could be overcome effectively.

Acknowledgments

Mahendra Kumar acknowledges the Irish Research Council, Ireland for awarding the IRC Postdoctoral Fellowship. The authors are thankful to Dr. Andreas Heise, School of Chemical Sciences and Dr. Ruth Larragy, School of Biotechnology, Dublin City University, Dublin, for giving permission to conduct the DSC and SDS-PAGE experiments, and to the National Centre for Sensor Research (NCSR) at DCU for access to analytical equipment. The authors are also grateful to Prof. Eoin Casey, School of Chemical and Bioprocess Engineering, University College of Dublin, Ireland for providing the facility to analyze the zeta potential of the membranes.

References

- 1 R. Baker, *Membrane technology and applications*, Wiley; New York, ed. **3**, 2012.
- 2 V. Orr, L. Zhong, M. Moo-Young and C. P. Cho, *Biotechnol. Adv.*, 2013, **31**, 450-465.
- 3 M. J. Santos, J. A. Teixeira and L.R. Rodrigues, *Sep. Purif. Technol.*, 2012, **90**, 133-139.
- 4 J. J. Lu, S. Wang, G. Li, W. Wang, Q. Pu and S. Liu, *Anal. Chem.*, 2012, **84**, 7001-7007.
- 5 B. Saha, J. Saikia and G. Das, *RSC Adv.*, 2013, **3**, 7867-7879.
- 6 C. Deng, Q. G. Zhang, G. L. Han, Y. Gong, A. M. Zhu and Q. L. Liu, *Nanoscale*, 2013, **5**, 11028-11034.
- 7 D. Yin and M. Ulbricht, *J. Mater. Chem. B*, 2013, **1**, 3209-3219.
- 8 L. J. Cheng and H. C. Chang, *Lab Chip.*, 2014, **14**, 979-987.
- 9 A. Doyen, C. C. Udenigwe, P. L. Mitchell, A. Marette, R. E. Aluko and L. Bazinet, *Food Chem.*, 2014, **145**, 66-76.
- 10 Y. Liao, T. P. Farrell, G. R. Guillen, M. Li, J. A. T. Temple, X. G. Li, E. M. V. Hoek and R. B. Kaner, *Mater. Horiz.*, 2014, **1**, 58-64.
- 11 A. Arunkumar and M. R. Etzel, *J. Membr. Sci.*, 2014, **454**, 488-495.
- 12 M. Kumar and M. Ulbricht, *RSC Adv.*, 2013, **3**, 12190-12203.
- 13 M. P. Sun, Y. L. Su, C. X. Mu and Z. Y. Jiang, *Ind. Eng. Chem. Res.*, 2010, **49**, 790-79.
- 14 N. J. Lin, H. S. Yang, Y. Chang, K. L. Tung, W. H. Chen, H. W. Cheng, S. W. Hsiao, P. Aimar, K. Yamamoto and J. Y. Lai, *Langmuir*, 2013, **29**, 10183-10193.
- 15 A. Schulze, M. F. Maitz, X. S. Shao, J. H. Li, Q. Zhou, J. Miao and Q. Q. Zhang, *J. Appl. Polym. Sci.*, 2013, **129**, 2472-2478.
- 16 H. Y. Yu, Y. Kang, Y. Liu and B. Mi, *J. Membr. Sci.*, 2014, **449**, 50-57.
- 17 R. Zimmermann, B. Marquardt, M. Fischer, C. Werner, M. Went and I. Thomas, *RSC Adv.*, 2013, **3**, 22518-22526.
- 18 J. Liu, X. Shen, Y. Zhao and L. Chen, *Ind. Eng. Chem. Res.*, 2013, **52**, 18392-18400.

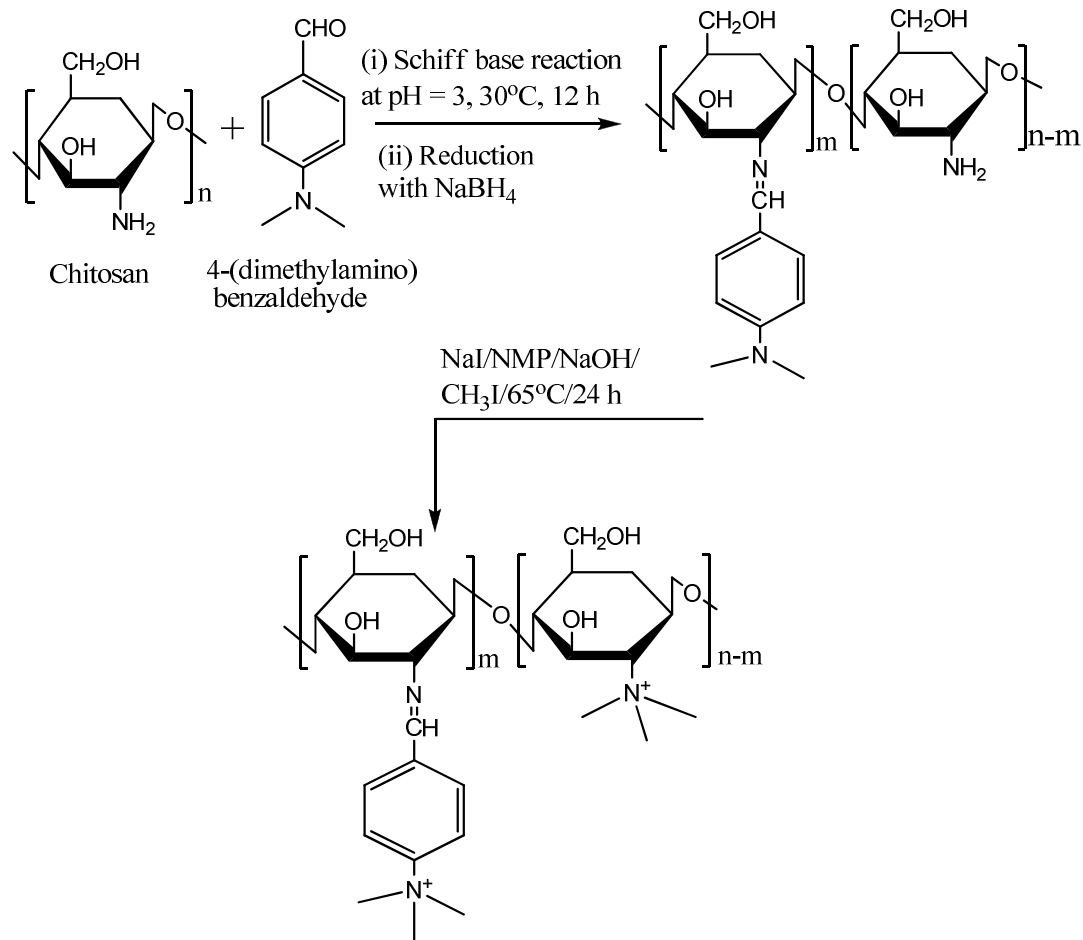
- 19 R. Kumar, A. M. Isloor, A. F. Ismail and T. Matsuura, *J. Membr. Sci.*, 2013, **440**, 140-147.
- 20 A. Mehta, and A. L. Zydney, *Biotechnol. Prog.*, 2006, **22**, 484-492.
- 21 A. Saxena, M. Kumar, B. P. Tripathi and V. K. Shahi, *Sep. Purif. Technol.*, 2010, **70**, 280-290.
- 22 B. Bolto, T. Tran, M. Hoang and Z. Xie, *Prog. Polym. Sci.*, 2009, **34**, 969-981.
- 23 T. Uragami, K. Okazaki, H. Matsugi and T. Miyata, *Macromolecules*, 2002, **35**, 9156-9163.
- 24 M. Kumar, M. A. Khan, Z. A. Allothman and M. R. Siddiqui, *Desalination*, 2013, **325**, 95-103.
- 25 J. Xue, W. Zhao, S. Nie, S. Sun and C. Zhao, *Carbohydr. Polym.*, 2013, **95**, 64-71.
- 26 X. Qiu, H. Yu, M. Karunakaran, N. Pradeep, S. P. Nunes and K. V. Peinemann, *ACS Nano*, 2013, **7**, 768-776.
- 27 A. Majhi and G. Pugazhenthii, *J. Chem. Technol. Biotechnol.*, 2010, **85**, 545-554.
- 28 P. Opanasopit, M. Petchsangsa, T. Rojanarata, T. Ngawhirunpat, W. Sajomsang and U. Ruktanonchai, *Carbohydr. Polym.*, 2009, **75**, 143-149.
- 29 M. Kumar, B. P. Tripathi and V. K. Shahi, *J. Membr. Sci.*, 2009, **340**, 52-61.
- 30 R. Heffernan, A. J. C. Semiao, P. Desmond, H. Cao, A. Safari, O. Habimana and E. Casey, *J. Membr. Sci.*, 2013, **448**, 170-179.
- 31 R. Ghosh and Z.F. Cui, *J. Membr. Sci.*, 1998, **139**, 17-28.
- 32 H. Guo, X. Li and D. D. Frey, *J. Chromatogr. A*, 2014, **1323**, 57-65
- 33 J. Hao, Y. Wu, J. Ran, B. Wu and T. Xu, *J. Membr. Sci.*, 2013, **433**, 10-16.
- 34 G. Socrates, *Infrared characteristic group frequencies*, Wiley; New York, 1980.
- 35 P. Y. Xu, K. Zhou, G. L. Han, Q. G. Zhang, A. M. Zhu and Q. L. Liu, *J. Membr. Sci.*, 2014, **457**, 29-38.

- 36 D. S. Kim, H. B. Park, J. W. Rhim and Y. M. Lee, *J. Membr. Sci.*, 2004, **240**, 37-48.
- 37 J. H. Cheng and T. S. Chung, *Chem. Eng. Sci.*, 2009, **64**, 5222-5230.
- 38 X. Feng, X. Wang, W. Xing, B. Yu, L. Song and Y. Hu, *Ind. Eng. Chem. Res.*, 2013, **52**, 12906-12914.
- 39 A. McKelvey and W. J. Koros, *J. Membr. Sci.*, 1996, **112**, 29-39.
- 40 S. G. Gholap, J. P. Jog and M. V. Badiger, *Polymer*, 2004, **45**, 5863-5873.
- 41 D. S. Kim, A. Labouriau, M. D. Guiver and Y. S. Kim, *Chem. Mater.*, 2011, **23**, 3795-3797.
- 42 E. Guler, Y. Zhang, M. Saakes and K. Nijmeijer, *ChemSusChem*, 2012, **5**, 2262-2270.
- 43 Q. Li, L. Liu, Q. Miao, B. Jin and R. Bai, *Chem. Commun.*, 2014, **50**, 2791-2793.
- 44 Z. Feng, Z. Shao, J. Yao, Y. Huang and X. Chen, *Polymer*, 2009, **50**, 1257-1263.
- 45 V. Valino, M. F. S. Roman, R. Ibanez and I. Ortiz, *Sep. Purif. Technol.*, 2014, **125**, 163-169.
- 46 M. Sorci, M. Gu, C. L. Heldt, E. Grafeld and G. Belfort, *Biotechnol. Bioeng.*, 2013, **110**, 1704-1713.
- 47 X. Zeng and E. Ruckenstein, *J. Membr. Sci.*, 1998, **148**, 195-205,
- 48 E. Celik, L. Liu and H. Choi, *Water Research*, 2011, **45**, 5287-5294.
- 49 A. Kosior, M. Antosova, R. Faber, L. Villain and M. Polakovic, *J. Membr. Sci.*, 2013, **442**, 216-224.
- 50 D. G. Kim, H. Kang, S. Han and J. C. Lee, *J. Mater. Chem.*, 2012, **22**, 8654-8661.
- 51 M. Kumar and M. Ulbricht, *J. Membr. Sci.*, 2013, **448**, 62-73.
- 52 D. Datta, S. Bhattacharjee, A. Nath, R. Das, C. Bhattacharjee and S. Datta, *Sep. Purif. Technol.*, 2009, **66**, 353-361.
- 53 C. L. Brooks, M. Morrison and M. J. Lemieux, *Protein Sci.*, 2013, **22**, 425-433.

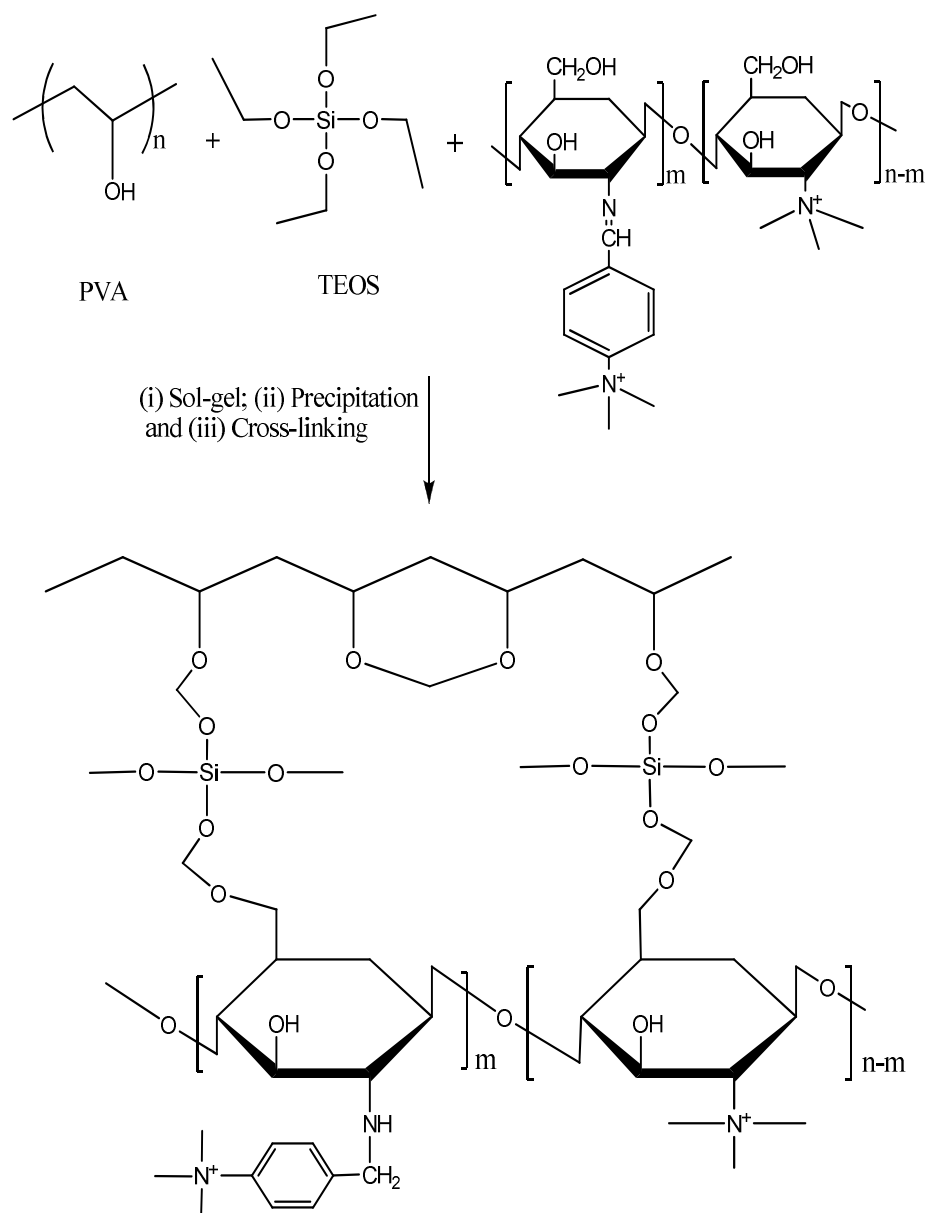
54 H. Y. Huang, T. J. Lo, Y. C. Chen, J. B. Hu and P. L. Urban, *Anal. Methods*, 2013, **5**, 5908-5911.

55 H. Wu, B. Tang and P. Wu, *J. Membr. Sci.*, 2010, **362**, 374-383.

56 Y. P. Lim and A. W. Mohammad, *Chem. Eng. J.*, 2010, **159**, 91-97.



Scheme 1. Reaction route for the preparation of methylated N-(4-N,N-dimethylaminobenzyl) chitosan by in situ quaternization using CH₃I and NaI at 65°C.



Scheme 2. Schematic reaction route for the preparation of positively charged organic-inorganic hybrid ultrafiltration membranes by the sol-gel and precipitation method.

Table 1. Physicochemical properties for the membranes with varied fraction of TMBC (%).

Membrane	Fraction of TMBC (%)	φ (%)	φ_f (%)	φ_b (%)	ε (%)	IEC (mequiv.g ⁻¹)	A _f (mequiv.g ⁻¹ H ₂ O)
A-0	-	44.8	33.5	11.3	50.9	-	-
A-10	10	52.5	30.9	21.6	58.5	0.46	0.87
A-20	20	57.7	27.1	30.6	63.1	0.55	0.95
A-40	40	64.4	21.7	42.7	66.7	0.70	1.09

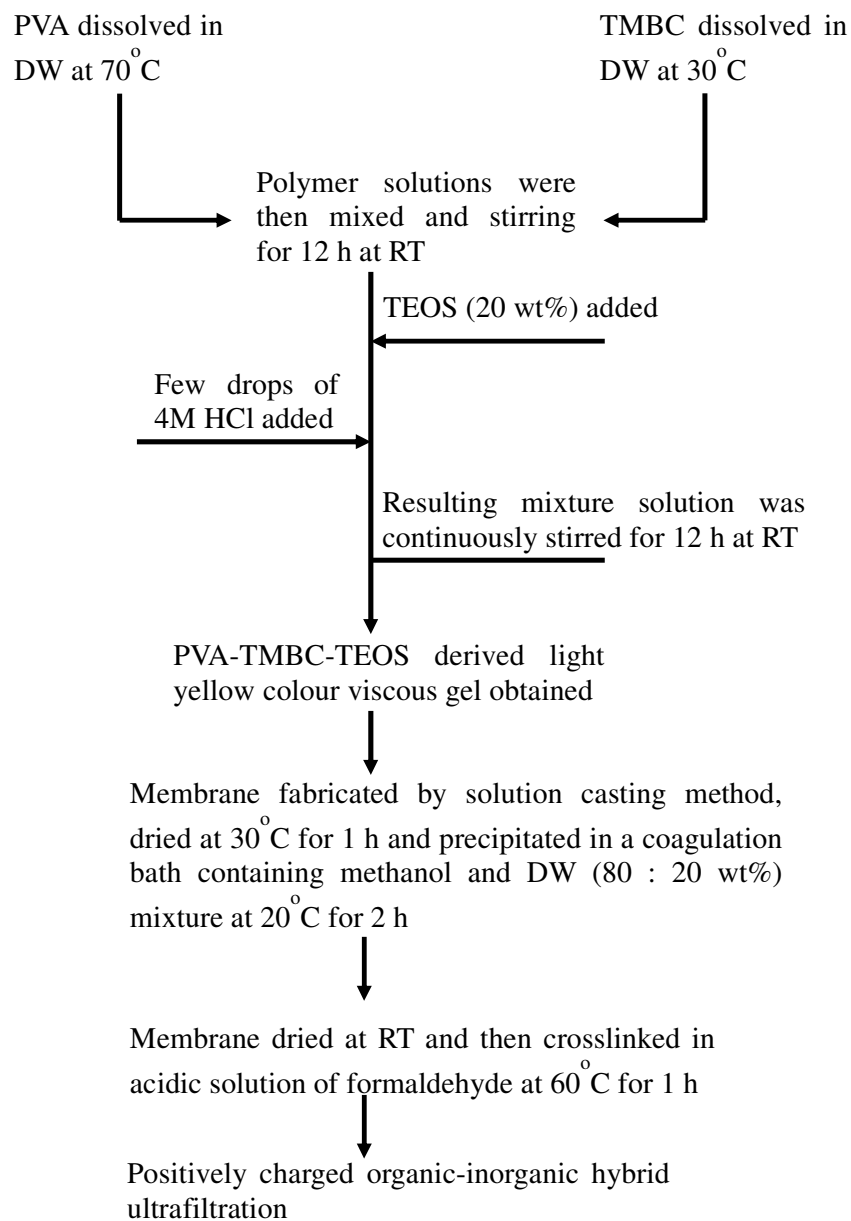


Fig. 1. Flow diagram for preparation of positively charged organic-inorganic hybrid ultrafiltration membrane.

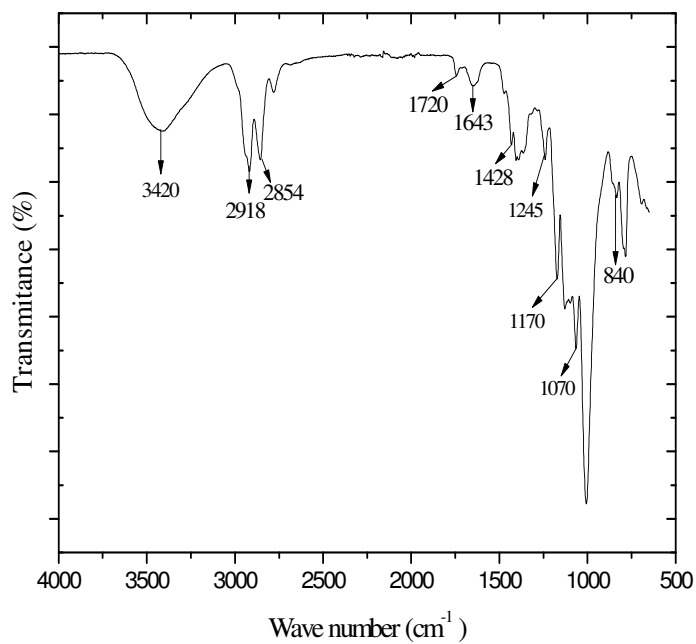


Fig. 2. ATR-FTIR spectrum for positively charged organic-inorganic hybrid ultrafiltration membrane A-40.

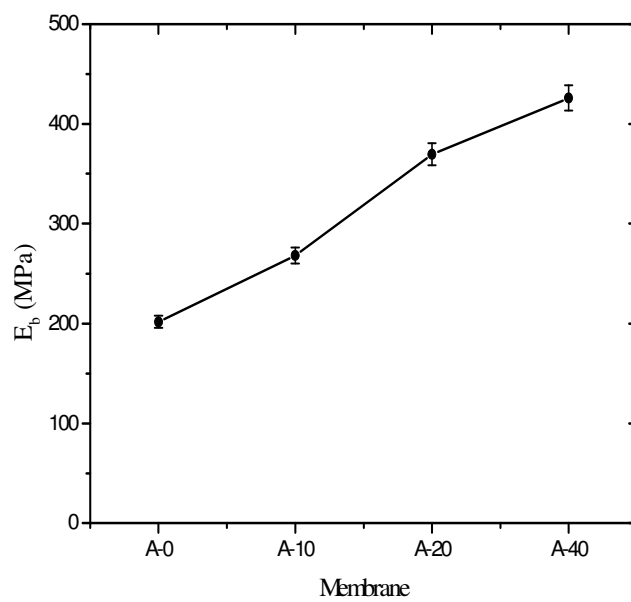


Fig. 3. The elongation value (E_b) at break for the membranes with varied fraction of TMBC (%).

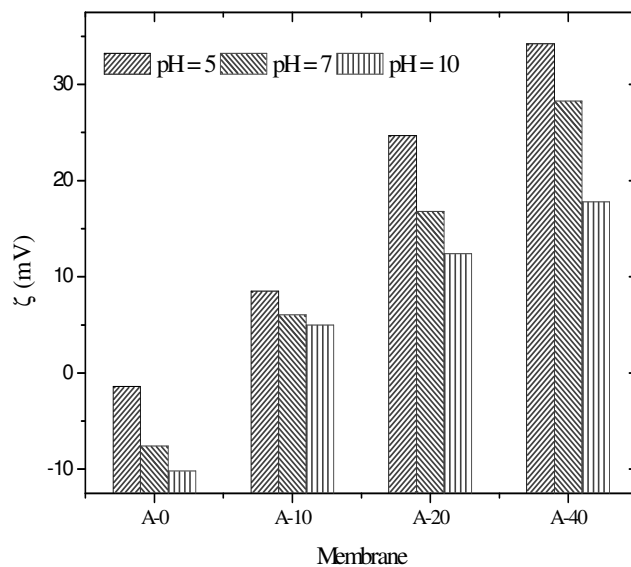


Fig. 4. The outer surface zeta potential values for the membranes with varied fraction of TMBC (%) at $pH = 5, 7$ and 10 .

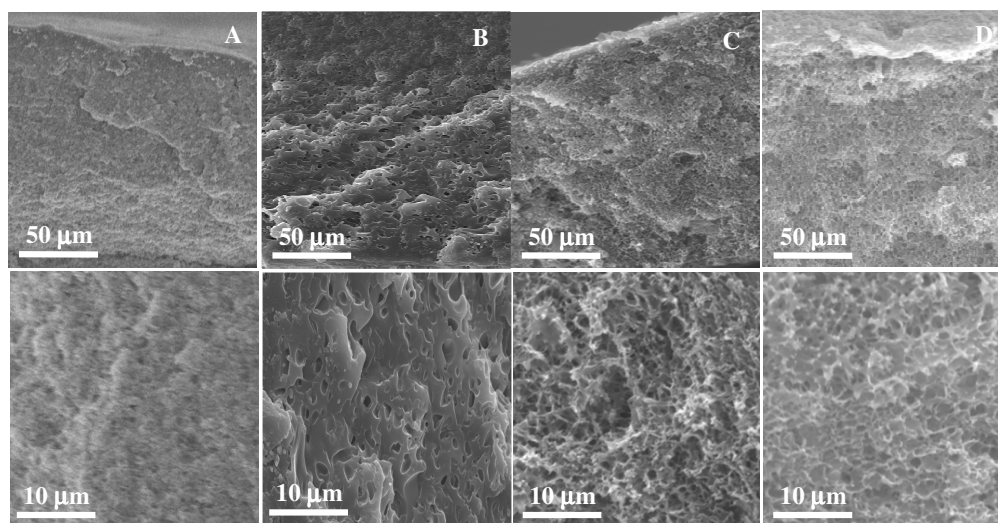


Fig. 5. Cross-section SEM images at high and low resolution for the membranes prepared with varied fraction of TMBC (cf. **Table 1**): (A) A-0; (B) A-10; (C) A-20 and (D) A-40.

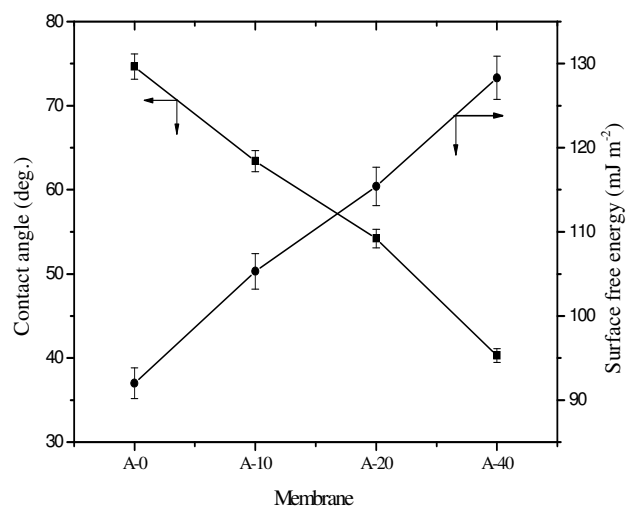


Fig. 6. Water contact angles and the surface free energy for the membranes with varied fraction of TMBC (%).

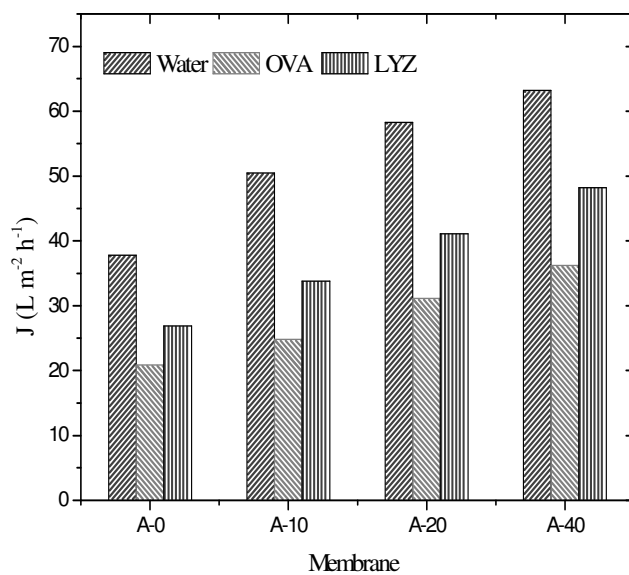


Fig. 7. Pure water flux and protein (OVA and LYZ) solution flux for the membranes at $pH = 7$, and 2 bar applied pressure with a stirring speed of 300 rpm.

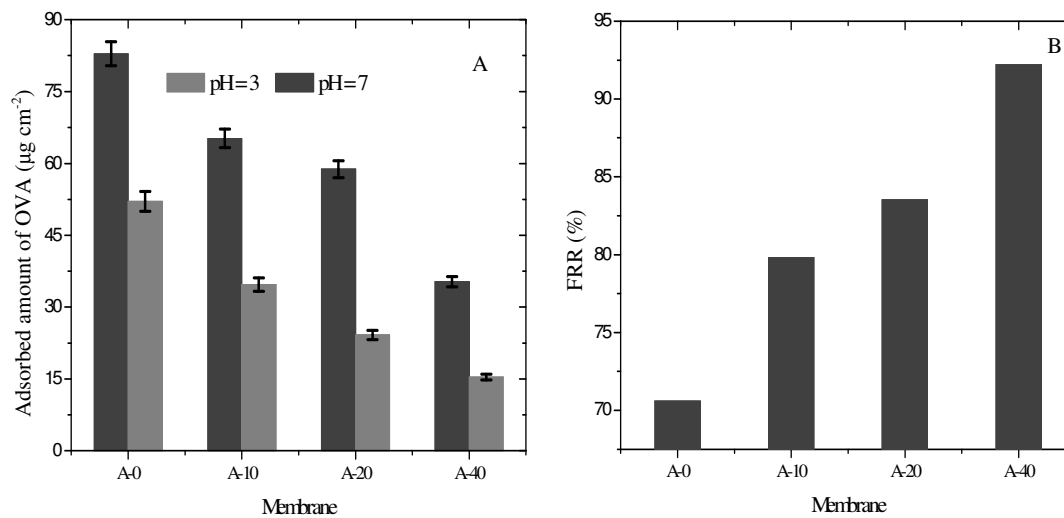


Fig. 8. (A) Adsorption of OVA at $pH = 3$ & 7 and (B) FRR values for the membranes after ultrafiltration of 500 ml solution of OVA (1 g L^{-1}) at $pH = 3$.

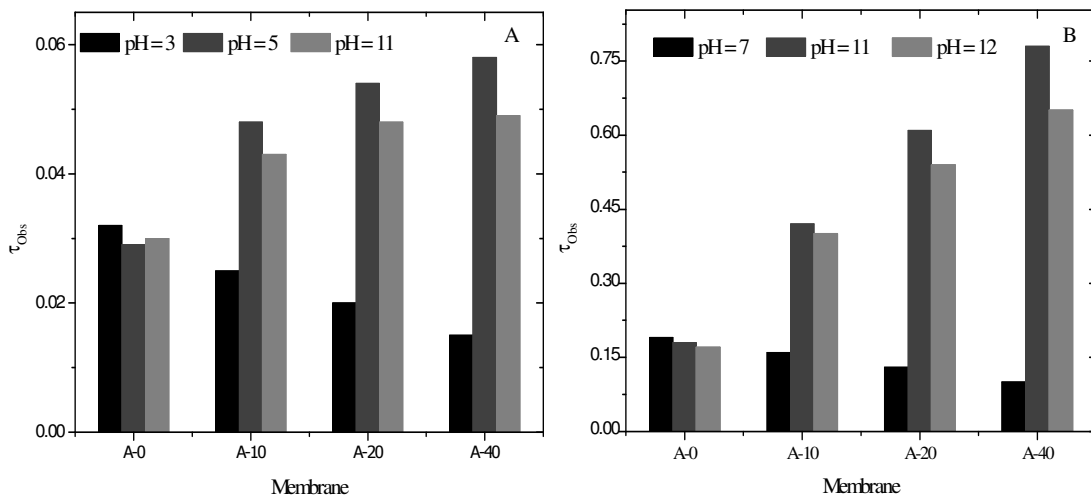


Fig. 9. Observed transmission (τ_{obs}) for: (A) OVA and (B) LYZ (1 mg ml^{-1} each) through the membranes at varied pH and 2 bar applied transmembrane pressure.

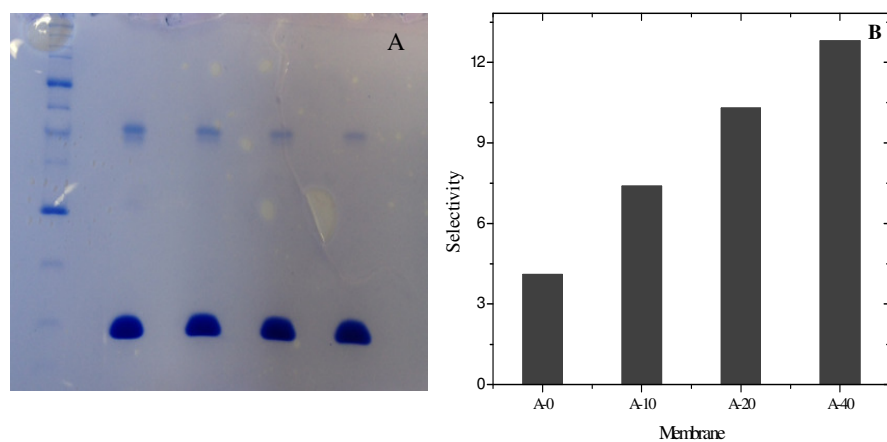


Fig. 10. (A) SDS-PAGE patterns for the permeate protein mixture solutions and (B) selectivity of the membranes towards LYZ versus OVA at $pH = 11$ and 2 bar applied transmembrane pressure.